JOURNAL OF MATERIALS SCIENCE 32 (1997) 3523–3534

Hydrothermal light-weight calcium phosphate cements: use of polyacrylnitrile-shelled hollow microspheres

T. SUGAMA
Energy Efficiency and Conservation Division, Department of Applied Science, Brookhaven National Laboratory, Associated Universities, Inc., Upton, Long Island, NY 11972, USA

B. LIPFORD
Alabama A&M University, Department of Physics, Normal, AL 35762, USA

Calcium phosphate cement (CPC) slurries with a very low density of less than 1.0 g cm^{-3} were prepared by incorporating polyacrylnitrile (PAN)-shelled hollow microspheres with calcite sizing into CPC pastes consisting of sodium metaphosphate, high alumina cement and water. Their characterizations were then investigated to assess their value as light-weight CPC cementing materials for use in geothermal wells at hydrothermal temperatures up to 300 °C. This light-weight cement showed the following four main features: firstly the chemical inertness of the PAN shells to CPC served to extend thickening time of the slurry; secondly the microsphere surfaces preferentially absorbed Al ions from among the various ionic species in the interstitial fluid of CPC at 100 °C, thereby forming amorphous Al-enriched sodium phosphate hydrates as interfacial intermediate layers which tightly linked the microspheres to the CPC matrix; thirdly although the thermal decomposition of PAN shells around 200 °C generated numerous voids in the cement body, these open spaces were filled by well-grown wardite crystals formed by the *in-situ* phase transformation of amorphous sodium aluminate phosphate hydrates, thereby preventing a serious loss in strength of the light-weight calcium phosphate cement (LCPC) specimens; fourthly the major phase composition of CPC matrix at 200 and 300 °C consisted of well-crystallized hydroxyapatite and boehmite compounds which can be categorized as alkali carbonation-resistant phases. The integration of these characteristics was responsible for maintaining the compressive strength of greater than 0.6 MPa for LCPC specimens derived from a very-low-density (0.98 g cm^{-3}) slurry exposed for 6 months to a 0.05 M Na_2CO_3-laden solution at 250 °C.

1. Introduction

One of the important considerations in designing a geothermal well-cementing slurry is that it should have a low density because slurries of normal density, 1.9–2.0 g cm^{-3}, used for completing geothermal wells frequently create the formation of voids and fractures in the underlying rock walls during cementing operations. Such undesirable fissures are formed by the significant hydrostatic pressures required to pump in very dense cement slurries. To solve this problem, cement slurries of low density are needed. Moreover, for cement binders to achieve a long service life as light-weight cementing materials, they must have a low rate of susceptibility to Na_2CO_3-related carbonation so that they can prevent total disruption of the cement-supported well structure caused by the attack of CO_2-containing brine on cements in geothermal wells at temperatures up to 300 °C [1, 2].

We previously investigated two potential high-temperature light-weight cementing systems, sodium metaphosphate (SMP) and sodium metasilicate (SMS), modified high alumina cements (HACs) containing a certain amount of aluminosilicate (mullite ($3Al_2O_3 \cdot 2SiO_2$))-shelled hollow microspheres (density of 0.67 g cm^{-3} and particle size of 75–200 μm) as one of the candidates for producing a cement slurry with a low density (less than 1.3 g cm^{-3}) [3, 4]. The major phases assembled in the SMP- and SMS-modified HAC pastes after autoclaving at 200 and 300 °C were identified as hydroxyapatite (HOAp) ($Ca_5(PO_4)_3(OH)$) and boehmite (γ-AlOOH) for the SMP system, and sodium calcium silicate hydrate ($Na_2Ca_2Si_2O_7 \cdot H_2O$) and γ-AlOOH for the SMS system. Hence, we expressed in terms of the calcium phosphate cement (CPC) for the former system and sodium calcium silicate cement (SCSC) for the latter system.

0022–2461

The resulting data suggested that the light-weight calcium phosphate cement (LCPC) and SCSC specimens derived from low-density (about 1.24 g cm^{-3}) slurries displayed good qualities after exposure for up to 10 days to 0.05 M Na_2CO_3-laden water at 200 °C, i.e., they had a compressive strength greater than about 5 MPa, water permeability of less than 1.5 mdarcies and a low rate of alkali carbonation of less than 0.5 wt%. However, considerable attention should be paid to the strong chemical affinity of the mullite shells to Na ions dissociated from the SMP and SMS aqueous solutions used as the cement-forming reactants and which had migrated from the surrounding Na_2CO_3 solution in the hydrothermal environments at elevated temperatures. The uptake of Na by the mullite microspheres led to the formation of an intermediate layer consisting of well-formed zeolite-type compounds as interfacial reaction products that precipitated in the critical boundary regions between the cement and microspheres. Although such a newly developed intermediate layer improves the adherence of the cement matrix to the microspheres, a major drawback was the decrease in effective thickness of the high-strength hollow microsphere shells caused by the hydrothermal-catalysed mullite–Na chemical interactions. This effect was directly reflected in the distribution of mechanically weak microspheres in the cement matrix phases, thereby resulting in a loss of strength. In fact, our most recent studies on the change in mechanical strength of the light-weight cement specimens after a 6 month exposure to a 0.05 M Na_2CO_3 solution at 250 °C demonstrated that compressive strengths of the LCPC and SCSC specimens were considerably reduced (0.49 versus 6.16 MPa for CPC, and 0.42 versus 3.56 MPa for SCSC), compared with unexposed specimens. No distinctive features of microspheres incorporated into the cement matrix was observed from the inspection of fractured surfaces of 6 month-exposed specimens by scanning electron microscopy (SEM), suggesting that the mullite shell–Na interaction is completed. Further, the SEM images showed that an excessive growth of crystalline zeolite-type phases as reaction products in the cement bodies caused the development of porous microstructure, and the generation of numerous microfissures, thereby resulting in a striking loss of strength and a marked increase in water permeability. Thus, the mullite-shelled hollow microspheres might be undesirable for use as light-weight fillers in alkali carbonation-resistant cement systems expected to be exposed to highly concentrated Na-ion-containing solutions under hot hydrothermal conditions.

The other ceramic microspheres, such as borosilicate glass and nepheline syenite, fared much worse than the mullite microspheres; namely, the hydrothermal reaction between these ceramics and the Na ions occurred very rapidly in Na_2CO_3 solution at 250 °C. Such a high rate of interaction introduced an exceptional growth of crystalline reaction products in the cement bodies, reflecting the development of sponge-like microstructure. As a result, there was a serious loss of strength in the light-weight cement specimens after a short exposure.

Based upon this information, our particular interest was to investigate the reactivity of the chemically inert organic polymer-shelled hollow microspheres with the Na ions and to assess their usefulness. The drawbacks of polymer-shelled microspheres are that they possess low mechanical strength and show thermal instability; however, their extremely low bulk density of around 0.1 g cm^{-3}, compared with that of ceramic-shelled microspheres is a worthwhile advantage; so it is important to assess the capability and feasibility of using polymer microspheres as a light-weight filler in preparing ultra-light-weight geothermal cements. For this aim, we employed commercial polyacrylnitrile (PAN)-shelled hollow microspheres having a bulk density of 0.13 g cm^{-3}. Also, CPC binder which has a higher strength than SCSC was used in this study.

To obtain detailed information on the characteristics of polymer-microsphere-filled light-weight CPC specimens after exposing them in an autoclave at 100, 200 and 300 °C, we focused on five objectives.

1. The thermal and hydrothermal characteristics of the microspheres themselves were established.
2. The changes in thickening time of slurries were investigated as a function of their density.
3. The elemental compositions of the reaction products formed by hydrothermal interactions between the microspheres and the interstitial solutions in the CPC slurry were studied, and the crystalline phases and compositions assembled in the microsphere-incorporated LCPC body after autoclaving were identified.
4. The development of microstructure in the autoclaved LCPC specimens was explored.
5. The compressive strength and water permeability of LCPC specimens autoclaved at 100, 200 and 300 °C were determined.

Finally, these data were integrated and correlated directly with changes in compressive strength of light-weight specimens after a long-term exposure to a 0.05 M Na_2CO_3-laden solution at 250 °C.

2. Experimental procedure

2.1. Materials

A 40 wt% SMP ($-(-NaPO_3-)-_n$) supplied by the Aldrich Chemical Company, Inc., was used as the cement-forming aqueous reactant to modify the HAC as the solid reactant. The HAC employed in this study was Secar 80 obtained from Lafarge Calcium Aluminates. The X-ray powder diffraction (XRD) data showed that the major chemical components of this HAC consisted of monocalcium aluminate (CA) ($CaO \cdot Al_2O_3$), calcium dialuminate (CA_2) ($CaO \cdot 2Al_2O_3$) and corundum (α-Al_2O_3). Commercial PAN-shelled hollow microspheres, called Dualite M6017 AE (DU) (Pierce & Stevens Corporation), were incorporated into the cement slurries as the light-weight filler. These microspheres had a bulk density of 0.13 g cm^{-3} and a particle size from 25 to 100 μm.

In preparing a low-density CPC slurry, all the three ingredients (HAC, microspheres and SMP solution)

were mixed thoroughly at room temperature. The slurry was then cast into cylindrical moulds of 30 mm diameter and 65 mm long to measure the compressive strength, and into discs of 30 mm diameter and 39 mm long to determine the water permeability. Following this, the moulds and discs were exposured in an autoclave at 100, 200 and 300 °C. Some light-weight specimens were immersed for up to 6 months into 0.05 M Na_2CO_3-laden water at 250 °C.

2.2. Measurements

Thermogravimetric analysis (TGA) and differential scanning calorimetry (DSC) were used to obtain information on the thermal decomposition of the polymer-based shell structure before and after autoclaving at 100, 200 and 300 °C. The thickening time of the slurry specimens was measured in accordance with API Schedule 4G Specification. The schedule corresponds to a simulated well of 1830 m depth at 50 °C under a pressure of 26.9 MPa. The test was completed when the consistency (BC value) of the slurry exceeded 70. The changes in the morphological features and elemental composition of the surfaces of the microspheres when they came in contact with an interstitial solution extracted from the CPC slurry at 100, 200 and 300 °C, were explored using SEM coupled with energy-dispersive X-ray analysis (EDXA). In preparing the interstitial fluids, the cement slurry consisting of 50 wt% HAC and 50 wt% (40 wt% SMP) solution was mixed thoroughly for 10 min with a magnetic stirrer at room temperature. The slurry was then separated by a centrifugal machine to obtain the aqueous phase. The concentration of ionic species present in aqueous phase was determined by atomic absorption (AA) spectrophotometry. The phase compositions formed in the microsphere-filled CPC bodies at hydrothermal temperatures of 100, 200 and 300 °C were identified by XRD. Correspondingly, the microstructure developed in the interfacial contact regions between the cement and microspheres was examined using SEM–EDXA techniques. The compressive strength of the LCPC cylinders was measured; the results given are the average value of three specimens. The disc-shaped specimens were used to obtain the data on the water permeability, utilizing a Ruska liquid permeameter under a pressure gradient of 2 atm.

3. Results and discussion

3.1. Thermal behaviours of microspheres

Before surveying the characteristics of the PAN-microsphere-incorporated light-weight cements, we investigated the thermal behaviour of the PAN-shelled hollow microspheres themselves before and after exposure for 24 h in autoclave at 100, 200 and 300 °C, using TGA and DSC. These measurements gave us data on the thermal stability and decomposition of $CaCO_3$-sized PAN shell structures. The TGA curve (Fig. 1), recorded in the temperature range 25–740 °C, showed a three-step decomposition process; there was a slight decrease in weight between

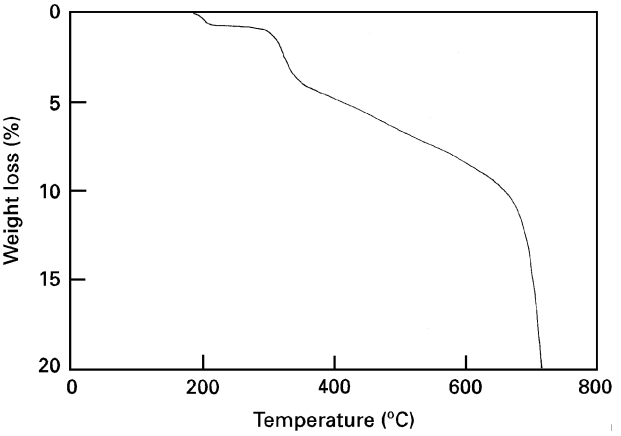

Figure 1 TGA curve for thermal decomposition of PAN-shelled microspheres in an air atmosphere at a rate of 10 °C min^{-1}.

about 175 and about 230 °C followed by a large decrease between about 275 and about 600 °C, and a considerable loss in weight between about 650 and 740 °C. The percentage weight loss at each individual stage was the following: about 0.8% up to 230 °C, about 7.7% between 275 and 600 °C, and about 11.7% between 650 and 740 °C.

In the study on the pyrolysis of bulk PAN polymer, Burlant and Parsons [5] reported that, below 210 °C, only ammonia was emitted as a gas phase during the thermal decomposition of PAN while, above this temperature, hydrogen cyanide (HCN) as the pyrolytic decomposition product evolved. Also, Manahan [6] found that the HCN in the presence of water was converted into ammonia and carbon monoxide through its hydrolysis pathway: $HCN + H_2O \rightarrow CO + NH_3$. Based upon this information, the first PAN decomposition stage, corresponding to the beginning at 175 °C, may be due to a weight loss caused by the emission of NH_3 from the PAN. The elimination of HCN seems to commence around 275 °C in the second stage. If this interpretation is correct, the onset of thermal decomposition of the PAN-shelled microspheres might occur at around 200 °C. Because the shell structure consists of the two phases, PAN as the underlying material and $CaCO_3$ as the sizing material of PAN surfaces, the sharp decline of the curve in the third stage may involve the thermal decomposition of $CaCO_3$, while the extent of degradation of the PAN shell is increasingly promoted with rising temperature. In fact, our TGA experiment with $CaCO_3$ as the chemical reagent gave us information that the onset of its decomposition is close to 600 °C.

To support the above information, next we attempted to compute by DSC the decomposition energy of PAN generated during the evolution of HCN for the microspheres autoclaved for 24 h at 100, 200 and 300 °C. On the assumption that the emission of HCN from PAN begins near 280 °C, the non-isothermal differential scanning calorimeter operated at constant heating rate of 10 °C min^{-1} in the temperature range 200–400 °C. The resulting DSC curve (Fig. 2) for all samples showed a typical endothermic feature as a function of temperature. The enclosed

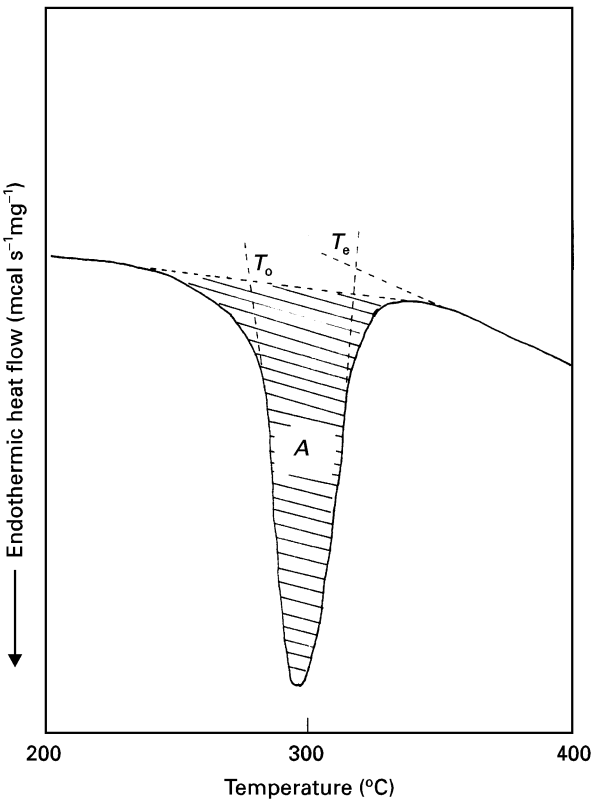

Figure 2 Non-isothermal DSC curve showing the total endothermic decomposition energy of microspheres.

area, A, of the curve with the baseline represents the total heat evolved during the endothermic decomposition. Thus, the total endothermic energy, ΔH (mcal mg^{-1}), can be computed using the following formula [7, 8]: $\Delta H = TRA/hm$, where T (°C in^{-1}) is the temperature scale, R (mcal s^{-1} in^{-1}) is the range sensitivity, A (in^2) is the peak area, h (°C s^{-1}) is the heating rate and m (mg) is the mass of the sample. Also, we determined the two temperatures at which the DSC curves show the onset (T_o) and end (T_e) of the endothermic decomposition; these temperatures were estimated from the curves by finding the intersection point of two linear extrapolations. Table I indicates the decomposition parameters of the microspheres before and after exposure in autoclaves at 100, 200 and 300 °C. The values of ΔH depended primarily on the hydrothermal temperatures; that is, its value is considerably reduced when the microspheres were treated at temperatures greater than 200 °C, while the value of 100 °C-treated microspheres was very close to that of unexposed microspheres. As mentioned in the discussion of the TGA curve, the emission of NH_3 as one of the decomposition compounds of PAN occurred near 175 °C. Correspondingly, the DSC data strongly suggested that almost all the PAN shell is decomposed during autoclaving for 24 h at 200 °C. The data also showed that the onset and end temperatures of the endothermic curve for all the samples ranged from 282 to 286 °C, and from 320 to 350 °C, respectively. Relating to the results from the TGA curve, it is apparent that the evolution of HCN from PAN takes place in this range of onset temperatures.

3.2. Light-weight cements

Table II shows the formulations of low-density CPC slurries used in this study, and their densities and thickening times. As shown in Fig. 3, the thickening time at the isothermal temperature of 50 °C is plotted as the elapsed time before the consistency reached a BC value of 70. The data revealed that the thickening time increases with a decrease in the density of slurry. In fact, a slurry with a density of 0.98 g cm^{-3}

TABLE II Formulation and density of microsphere-filled CPC slurries

SMP solution (wt%)	HAC (wt%)	DU (wt%)	Density (g cm^{-3})	Thickening time (min)
44.0	53.0	3.0	1.32	40
46.5	50.0	3.5	1.22	45
48.0	48.0	4.0	1.13	54
50.0	45.5	4.5	1.06	96
51.0	44.0	5.0	1.00	111
52.0	42.5	5.5	0.98	125

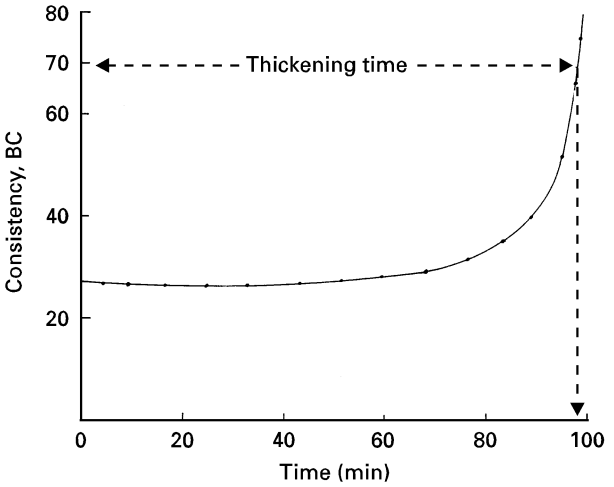

Figure 3 Changes in the consistency of LCPC slurry as a function of time.

TABLE I Decomposition parameters for PAN-shelled microspheres before and after exposure for 24 h in an autoclave at 100, 200 and 300 °C

Treatment temperature (°C)	Onset temperature T_o (°C)	End temperature T_e (°C)	Total endothermic energy ΔH (mcal mg^{-1})
25	285	340	2.85
100	282	340	2.78
200	284	320	0.12
300	286	350	0.08

had a thickening time of about 125 min, corresponding to 80 min more than that of the 1.32 g cm^{-3} density slurry.

Using the mullite-shelled microspheres, our previous study on determining the thickening time of microsphere-containing CPC slurry showed that a strong chemical affinity of microsphere with cement caused the reduction in its thickening time [3]. However, the PAN-shelled microspheres had no such influence on thickening time, suggesting that, even though they have some reactivities with cement, the extent might be much smaller than that of the mullite.

To assess the extent of reactivity of the $CaCO_3$-sized PAN shell surfaces with the cements at temperatures up to 300 °C, we explored the changes in morphological feature and elemental composition of the microsphere surfaces after exposure for 24 h in the interstitial fluids extracted from the slurry at 100, 200 and 300 °C, respectively, by SEM coupled with EDXA. The concentration of ionic species present in the CPC fluids determined by AA was as follows: Ca, 2.0 μg ml^{-1}; Na, 1.7×10^2 μg ml^{-1}; Al, 2.2×10^{-4} μg ml^{-1}; Si, 1.0 μg ml^{-1}; P, 1.3×10^2 μg ml^{-1}. Fig. 4a shows the scanning electron micrograph for the as-received microsphere surfaces and Fig. 4c the

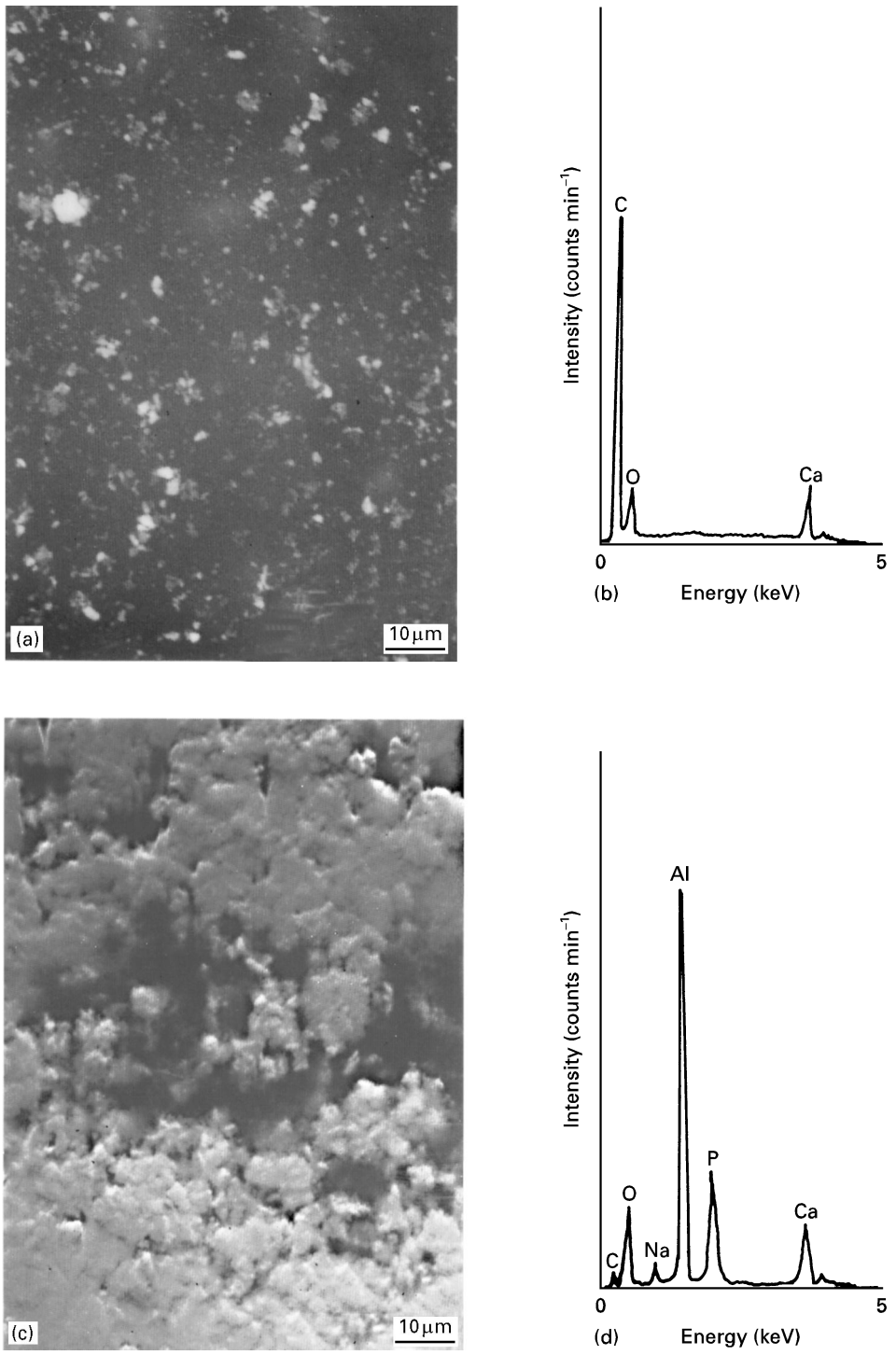

Figure 4 (a), (c) Scanning electron micrographs and (b), (d) energy-dispersive X-ray spectra of (a), (b) as-received microspheres and (c), (d) microsphere surfaces treated with interstitial fluids of cement slurry at 100 °C.

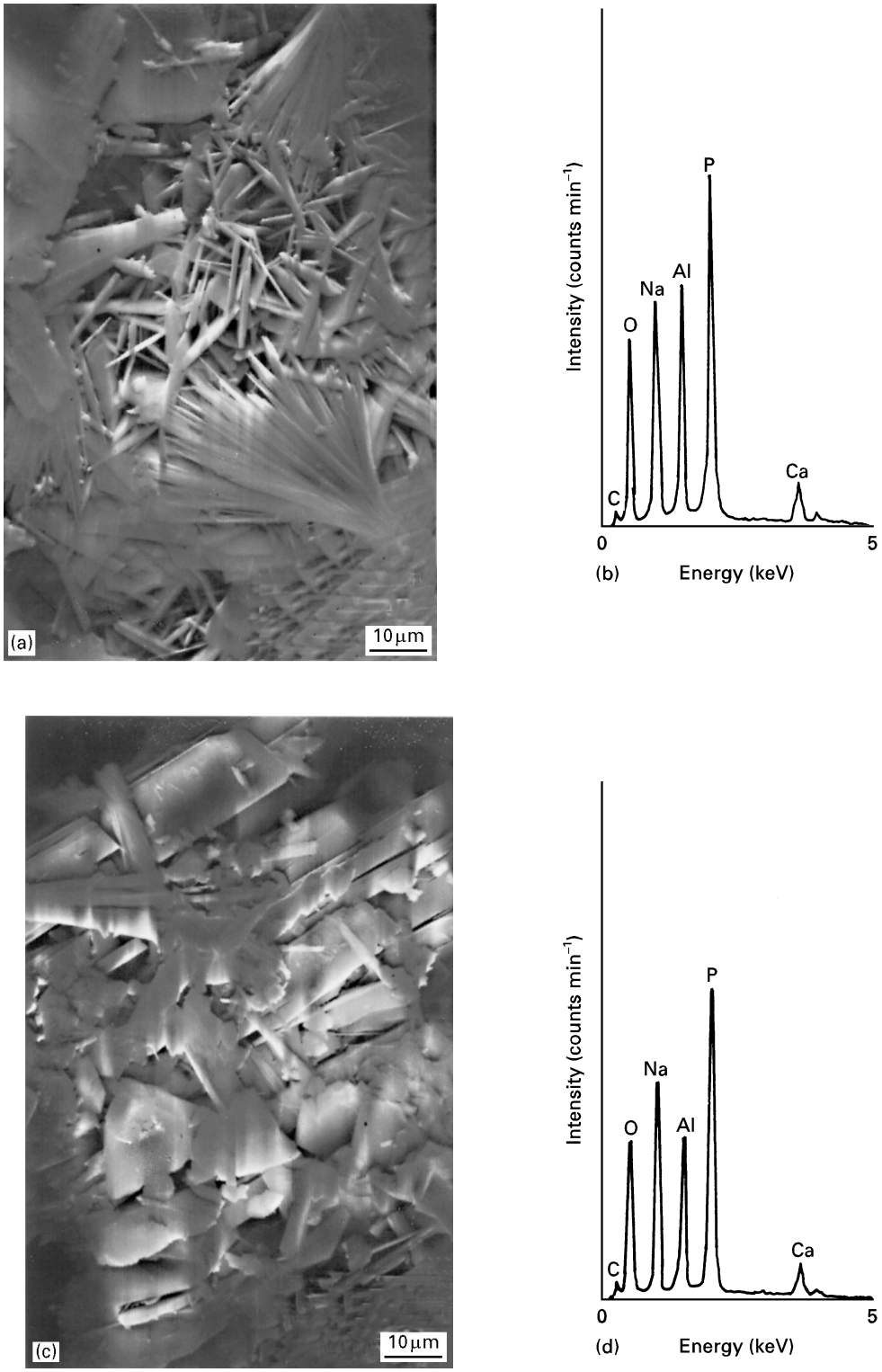

Figure 5 SEM–EDXA data of microsphere surfaces treated with cement–interstitial fluids at (a), (b) 200 °C and (c), (d) 300 °C.

microsphere surfaces after exposure in the CPC fluids at 100 °C. The original surfaces of the microspheres were changed into a rough morphological feature caused by the coverage of chemical compounds precipitated on them. The energy-dispersive X-ray spectrum (Fig. 4b) accompanying SEM for the untreated microsphere surfaces revealed the presence of only three elements, carbon, oxygen and calcium, originating from the underlying PAN shell and the $CaCO_3$ sizing. Also, we noted that numerous particles distributed randomly over the PAN shell surfaces were due to the $CaCO_3$ sizing because of a marked growth of Ca and O peaks in the energy-dispersive X-ray pattern (not shown). Interest was then focused on the energy-dispersive X-ray spectrum taken from the precipitates that covered the microspheres at 100 °C (Fig. 4d); it showed that the precipitates have a most intense line of Al, a moderate line for O, P and Ca, and weak C and Na peaks. Although the concentration of the Al ion in the interstitial fluid was lower than that of the other ionic species, the presence of Al as the principal line strongly suggested that the microspheres

preferentially absorb the Al ion, rather than Na, P and Ca ions. A striking decay of the line intensity of C compared with that of the untreated microspheres is the embodiment of the thick coverage of massive precipitates over the shell surfaces. Increasing the temperature to 200 °C caused a dramatic change in morphological features and also in aspects of the energy-dispersive X-ray spectrum. The former, as shown in Fig. 5a and b, was characterized by converting the bulky amorphous-like structure of precipitates formed at 100 °C into an interlocking texture of thin plate-like crystals. Such an amorphous → crystal phase conversion resulted in a remarkable change in the elemental composition of precipitates. As is evident from the energy-dispersive X-ray spectrum of plate-like crystals, the Al signal as the principal element in the amorphous precipitates formed at 100 °C was replaced by an intensive P signal during exposure at 200 °C, while the Al, Na and O elements become the secondary signals. Nevertheless, many P, Al and Na ions appear to migrate from the fluid phase to the surfaces of the microspheres. In contrast, the signal intensity of Ca tends to decrease with increasing temperature. This finding strongly demonstrated that almost all the Ca signal seems to be ascribable to that of the $CaCO_3$ sizing. If this interpretation is correct, the Na, Al and P ions in the fluids at 200 °C preferentially migrate to the surfaces of the microspheres to precipitate crystalline sodium aluminium phosphate compounds. However, it is very difficult from energy-dispersive X-ray spectra to estimate the extent of the chemical affinity of the $CaCO_3$ sizing with these ionic species. Formation of this crystal was observed on the 300 °C-treated microspheres (Fig. 5c), while the energy-dispersive X-ray spectral aspects (Fig. 5d) remained almost the same as those for 200 °C-treated spheres, except that the signal intensity of Al was somewhat weaker, compared with that at 200 °C. As a result, the phase transitions of chemical compounds precipitated on the microspheres as a function of temperature can be interpreted in the following way; when the microspheres came in contact with the CPC fluids at 100 °C, the Al ions preferentially migrated from the fluid phase to their surfaces to form an amorphous Al-enriched sodium phosphate compound. Increasing the temperature to 200 °C promoted the migration of a large number of Na and P ions to the microspheres. The uptake of these ions by the microspheres led to the amorphous → crystalline sodium aluminium phosphate phase transformation. Because thermal decomposition of the shells of the microspheres begins near 180 °C, it is believed that this phase transformation takes place in conjunction with the undermining actions of the underlying microspheres. A further increase in temperature to 300 °C resulted in the formation of well-crystallized sodium aluminium phosphate compounds.

These findings were supported by investigating the phase identification and *in-situ* phase transformation of the LCPC as a function of temperature, and also exploring the microstructure developed in the autoclaved LCPC bodies. To gain this information, cylindrical specimens (of 30 mm diameter and 60 mm length) of the LCPC derived from the slurry with the lowest density of 0.98 g cm^{-3} were exposed for 24 h in the hydrothermal environments at temperatures up to 300 °C. After exposure, the specimens were dried for 24 h in an oven at 110 °C and then were crushed to a size of less than 0.074 mm for XRD analysis. Also, a fractured surface of these dried specimens was examined by SEM–EDXA.

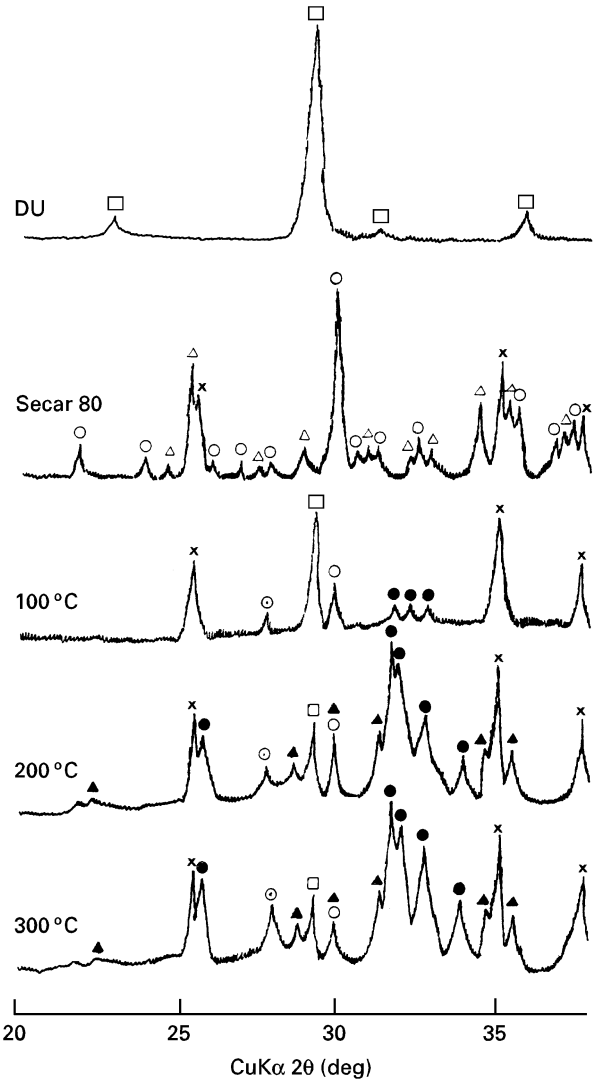

Figure 6 XRD tracings of as-received microspheres (DU), HAC (secar80), and LCPC specimens autoclaved at 100, 200 and 300 °C. (□), $CaCO_3$; (○), CA; (△), CA_2; (×), α-Al_2O_3; (⊙), γ-AlOOH; (●), HOAp; (▲), $NaAl_3(PO_4)_2(OH)_4 \cdot 2H_2O$.

An XRD tracing, ranging from 0.225 to 0.127 nm, was made for LCPC specimens autoclaved at 100, 200 and 300 °C. For the comparison purposes, the as-received microspheres and unhydrated HAC were also used as the reference samples. The results from these powder samples are given in Fig. 6. From the XRD data, the major crystalline phase of the microspheres (DU) as reference sample appears to be the calcite ($CaCO_3$) as the sizing material of the PAN-based shell surfaces. HAC (Secar80) as the other reference sample had multiphases consisting of CA, CA_2 and α-Al_2O_3. When the LCPC was exposed in autoclave at 100 °C, the particular features of the XRD pattern compared with those of these reference samples, were as follows:

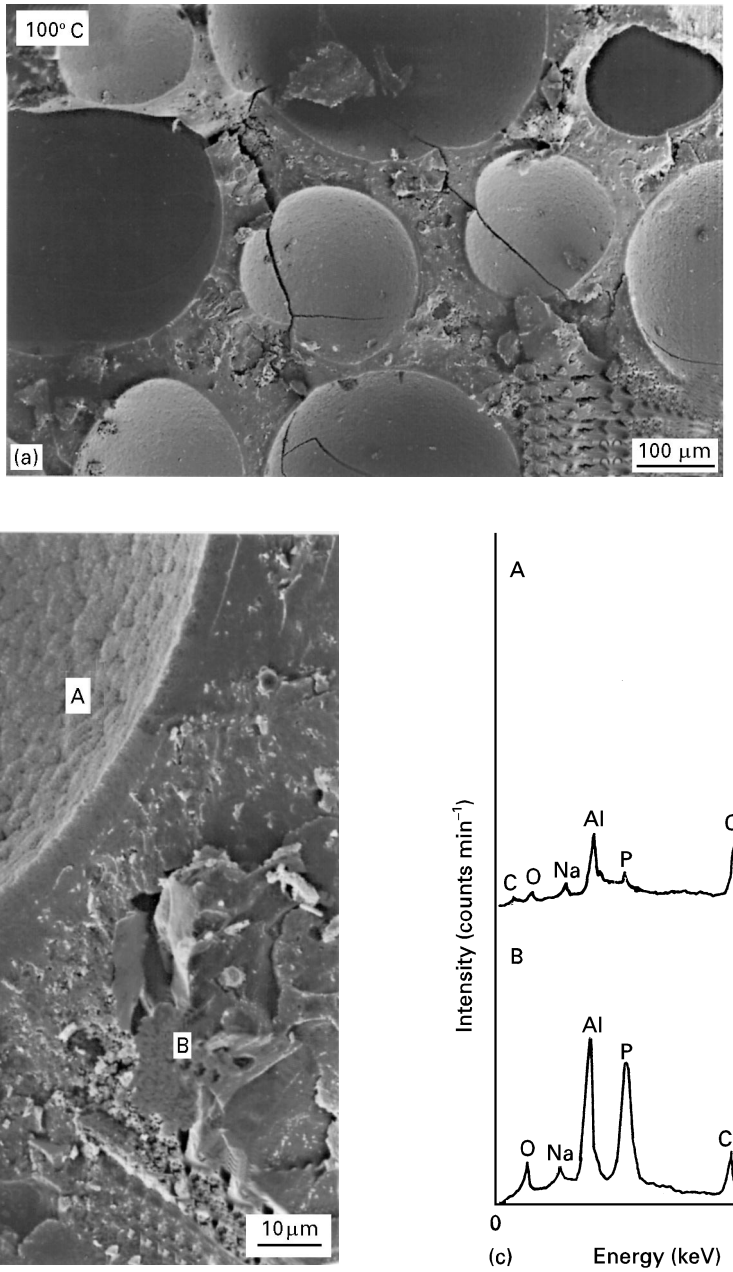

Figure 7 SEM images coupled with energy-dispersive X-ray spectra for fractured surfaces of 100 °C-autoclaved LCPC specimens.

1. the development of two new crystalline phases, γ-AlOOH and HOAp;
2. the elimination of CA_2-related *d* spacings;
3. a striking decay of the $CaCO_3$- and CA-associated line intensities;
4. a remaining intense signal of α-Al_2O_3.

Referring to the findings 1–3, it is conceivable that the formations of γ-AlOOH and HOAp were synthesized through hydrothermal-catalysed reactions between CA_2, CA or $CaCO_3$ and SMP reactants. However, α-Al_2O_3 which is one of the chemical components of the HAC reactant seems to be chemically inert to the SMP, thereby resulting in the finding 4. Increasing the temperature to 200 °C led to a striking growth of HOAp-related *d* spacings in conjunction with the appearance of new crystal phase, reflecting the formation of wardite ($NaAl_3(PO_4)_2(OH)_4 \cdot 2H_2O$). We noted earlier that the interaction between the CPC fluids and microspheres at 200 °C introduced sodium aluminium phosphate compounds as precipitates onto the surfaces of the microspheres. Thus, this precipitate is likely to be associated with the wardite phase. The pattern also demonstrated that the rate of reaction of $CaCO_3$ with the SMP is further promoted when the hydrothermal temperature was increased to 200 °C because of the loss of its *d* spacings. Thus, the decomposition of microspheres in the cement bodies not only is due to the thermal degradation of PAN shell occurring near 200 °C but also may be caused by the interaction of $CaCO_3$ with SMP. At 300 °C, the pattern closely resembled that of the 200 °C-autoclaved specimens, except for a further reduction in $CaCO_3$-related line intensity. Hence, the phase compositions assembled in the LCPC at temperatures above 200 °C were HOAp and unreactive α-Al_2O_3 as the major phases, with wardite, γ-AlOOH, $CaCO_3$ and CA as secondary phases.

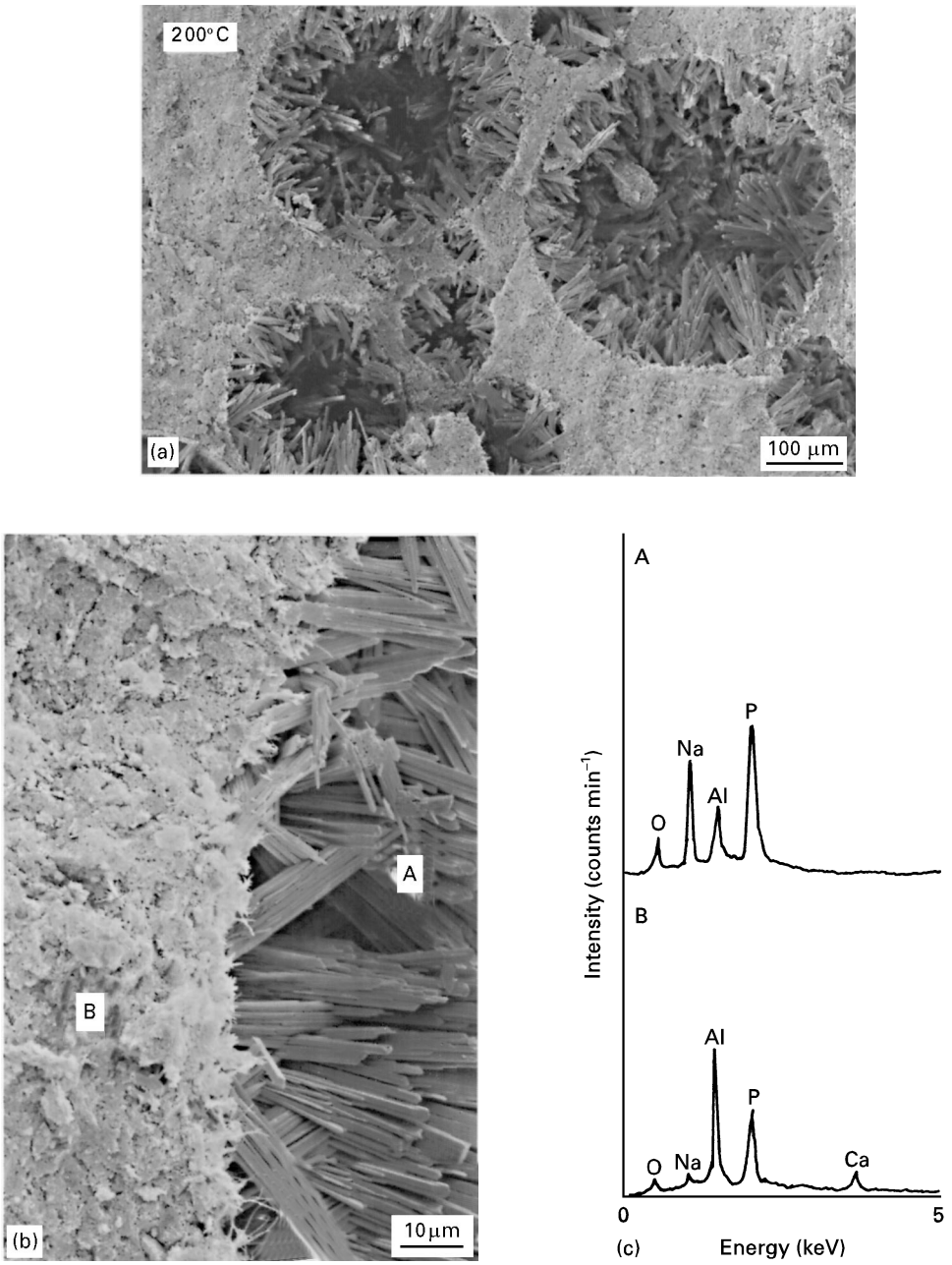

Figure 8 SEM–EDXA for fractured surfaces of 200 °C-autoclaved LCPC specimens.

To visualize and substantiate this information further, we explored the fractured surfaces of autoclaved LCPC specimens by SEM–EDXA. Fig. 7 shows scanning electron micrographs, together with the energy-dispersive X-ray spectrum of the 100 °C-autoclaved specimens. As seen in Fig. 7a, the failure seems to propagate through the microspheres, suggesting that the adherence of the CPC matrix to the microspheres is excellent. In fact, a dense structure made up of the intermediate layers can be observed in the critical interfacial-boundary regions between the matrix and microspheres (see the enlarged SEM image in Fig. 7b). From the EDXA at the location denoted A, the surface chemical composition of microspheres separated from the matrix involved Ca and Al as the major components, and P, Na, O and C as the minor components. Because the major contributor to the three elements Ca, C and O is probably $CaCO_3$, the microspheres preferentially absorbed Al, rather than the other cement-related elements. This was in agreement with the energy-dispersive X-ray spectrum of the microspheres treated with the CPC fluids at 100 °C (see Fig. 4d). Energy-dispersive X-ray examinations of site B at a distance of about 20 μm from the edge of microsphere revealed an elemental distribution with Al and P as the most intense peaks, secondary strong Ca and O peaks, and a smaller Na peak. Relating these findings to the results from the XRD study, all the elements, except for Na, may belong to the unreactive α-Al_2O_3 and CA, and the γ- AlOOH and HOAp reaction products formed in the cement matrix. A dramatic alteration in morphological features was observed for the 200 °C-autoclaved specimens (Fig. 8a). There were two specific differences from the 100 °C-autoclaved specimens; one is the disappearance of the microspheres, and the other was the growth of

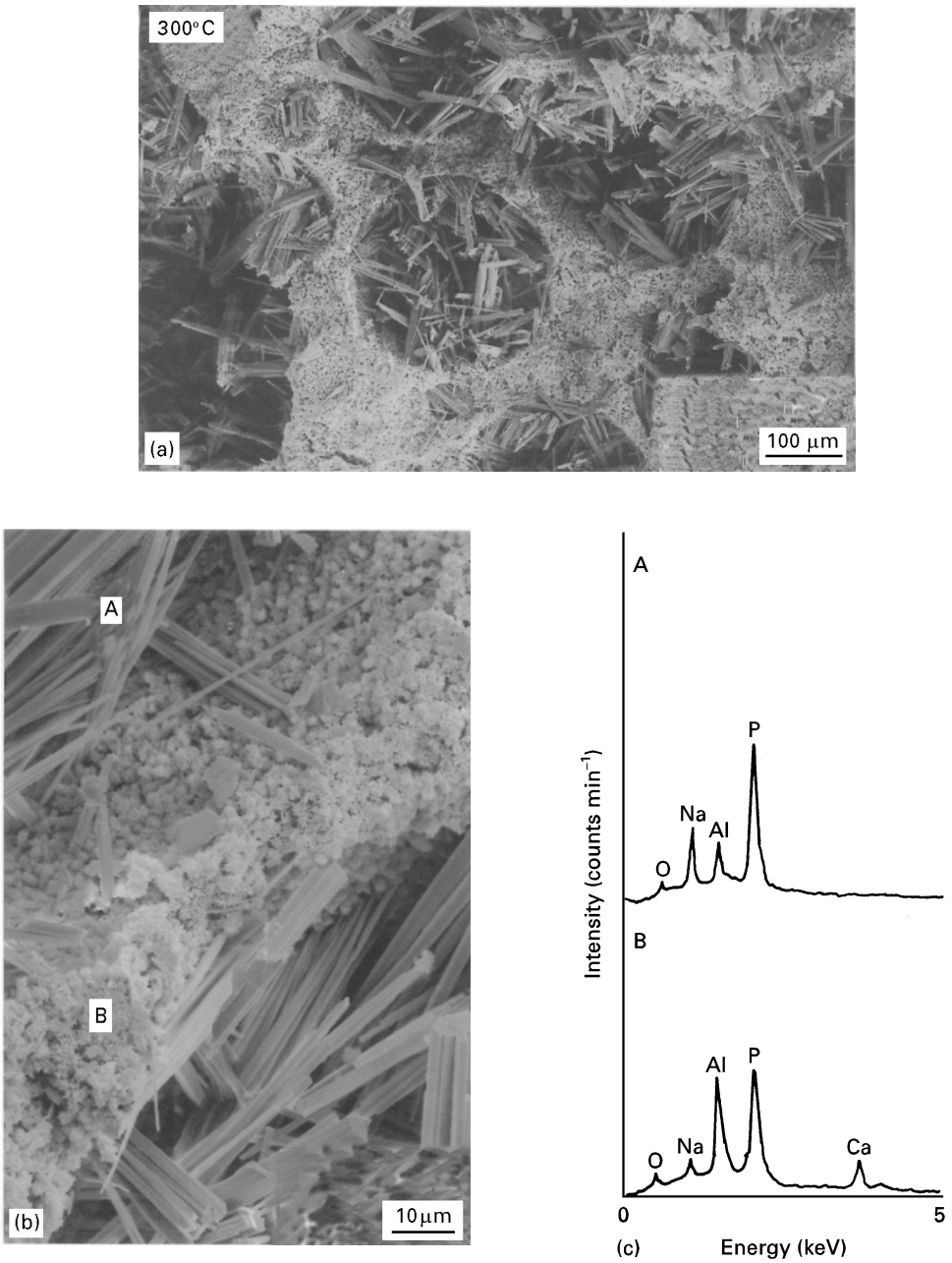

Figure 9 SEM–EDXA data taken from fractured surfaces of 300 °C-autoclaved LCPC specimens.

needle-like crystals in the pore spaces created by decomposing the PAN shell of the microspheres. An enlargement of a portion of the interfacial area (Fig. 8b) disclosed the microstructure in which a well-grown crystal was embedded in the matrix layers. The energy-dispersive X-ray spectrum of crystals denoted as A had four elements, O, Na, Al and P; no Ca was detected. Relating to the XRD data described earlier, the needle-like crystals are attributable to the formation of wardite. The energy-dispersive X-ray spectral features taken from the location B in the matrix were similar to those of the matrix formed in the 100 °C-autoclaved specimens. As shown in Fig. 9, an elevated temperature of 300 °C seems to promote further growth of wardite crystals. Although such crystal growth fills the voids created by the disappearance of the microspheres, the internal stresses generated by its excessive growth may cause the development of microcracks in the cement matrix phases, thereby leading to the formation of a porous structure. No significant differences between the energy-dispersive X-ray spectra of wardite indicated as A and the matrix B from those for the 200 °C-autoclaved specimens was found (Fig. 9c), suggesting that the phase composition at 300 °C is almost the same as that at 200 °C.

All the data described above were correlated directly with the changes in compressive strength and water permeability of LCPC specimens autoclaved at 100, 200 and 300 °C as a function of density of their slurries. The compressive strength–slurry density relation, as depicted in Fig. 10, indicated that the strength depended primarily on two parameters: the hydrothermal temperature and slurry density. Regarding the former parameter, the increase in temperature caused a loss in strength. This loss is perhaps due to the decomposition of microspheres in conjunction

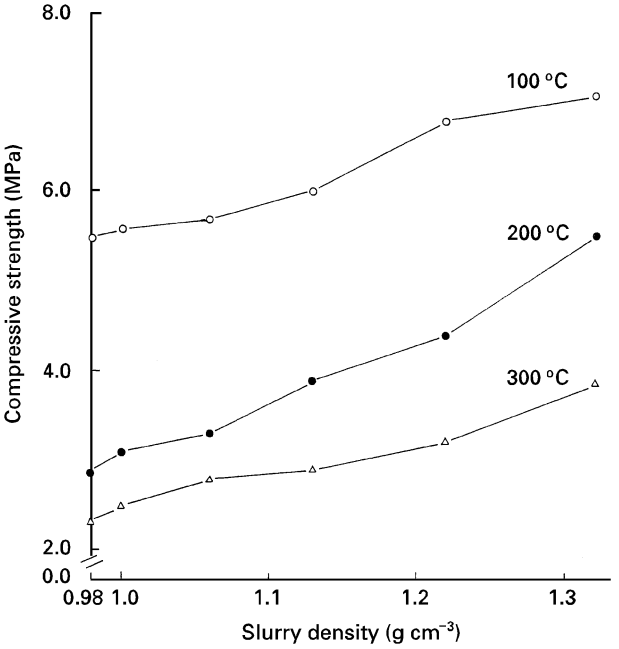

Figure 10 Changes in compressive strength of LCPC specimens autoclaved at 100, 200 and 300 °C as a function of slurry density.

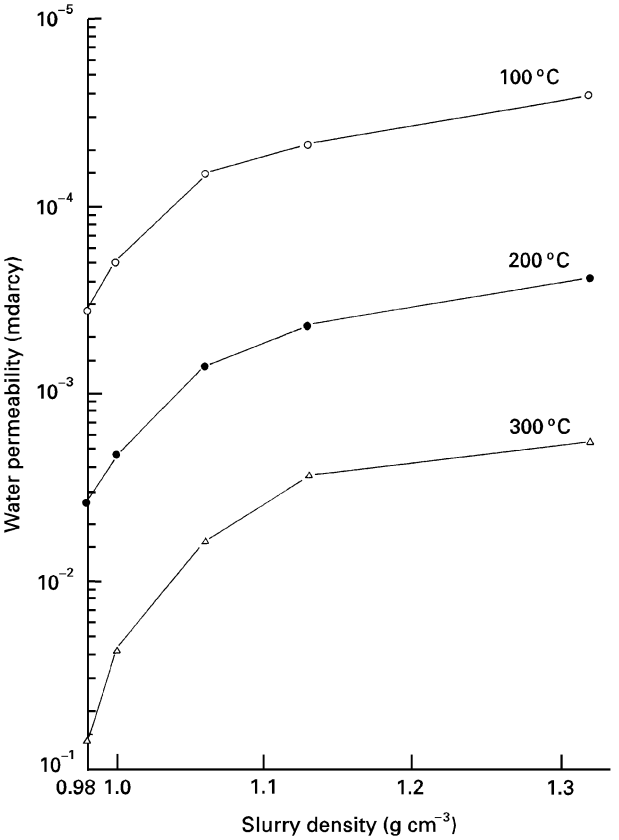

Figure 11 Variation in water permeability of LCPC specimens autoclaved at 100, 200 and 300 °C as a function of slurry density.

with an exceptional growth of wardite crystals. However, considering that the needle-like wardite crystals have a favourable effect, growing into the voids created by decomposition of the microspheres, we assumed that the filling up of numerous voids by a moderately grown crystal might reinforce a defective LCPC structure, thereby minimizing the decrease in strength. As expected, the development of strength for specimens derived from a low-density slurry was poor. Nevertheless, specimens prepared from the slurry with a very low density of 0.98 g cm^{-3} had compressive strengths of 5.5, 2.9 and 2.3 MPa at temperatures of 100, 200 and 300 °C, respectively. Correspondingly, the water permeability increased with increasing temperature and decreasing slurry density (Fig. 11). Hence, we believe that the increased water permeability at elevated temperatures is due to the same reasons as described for the loss of strength.

TABLE III Changes in the compressive strength of LCPC specimens after long-term exposure in 0.05 M Na_2CO_3-laden solution at 250 °C

Slurry density (g cm^{-3})	Compressive strength (MPa)			
	0 month	1 month	3 months	6 months
1.32	4.65	2.88	1.93	1.67
1.06	3.02	1.97	1.07	0.91
0.98	2.51	1.06	0.71	0.68

Next, our attention focused on determining the changes in compressive strength for the LCPC specimens after exposure for up to 6 months to a 0.05 M Na_2CO_3-laden solution at 250 °C. The LCPC specimens used to investigate the susceptibility to hot alkali carbonation were derived from the low-density slurries of 1.32, 1.06 and 0.98 g cm^{-3}. The results from these specimens are given in Table III. The strengths of unaged specimens (0 months) correspond to those determined from specimens exposed for 24 h to water at 250 °C. As seen, there is a rapid loss in strength for all the specimens exposed for between 1 and 3 months. After 6 months, there was only a further slight reduction in strength, compared with that of the specimens aged for 3 months. However, there is no evidence to show why a significant reduction in strength occurs in the first month. To answer this question, we are currently examining the rate of alkali carbonation, the phase composition and microstructural development of Na_2CO_3-exposed specimens. Results of these investigations will be reported separately.

4. Conclusion

The incorporation of PAN-shelled hollow microspheres with a bulk density of 0.13 g cm^{-3} into CPC slurries consisting of SMP, HAC and water offered the possibility of designing the slurries with a very low density of less than 1.0 g cm^{-3}. Although the calcite-sized layer existing at the outer surface of the PAN shell had a certain rate of reactivity with the CPC, the chemical inertness of the PAN shell to the SMP played an important role in extending the thickening time of low-density CPC slurries containing a large number of microspheres. When the microspheres came into contact with an interstitial solution of CPC pastes at 100 °C, their surfaces preferentially absorbed Al ions rather than Ca, P and Na ions. This uptake of Al by the microspheres promoted the precipitation of amorphous Al-enriched sodium phosphate hydrate onto the microsphere surfaces. This hydrate product

formed in the critical interfacial boundary regions between the microspheres and CPC matrix provided the formation of intermediate transition layers which tightly link the microspheres with the matrix. Increasing the hydrothermal temperature to 200 °C led to the *in-situ* conversion of this amorphous hydrate phase into a crystalline sodium aluminium phosphate hydrate phase called wardite ($NaAl_3(PO_4)_2(OH)_4 \cdot 2H_2O$). Although the thermal decomposition of PAN shells near 200 °C created numerous voids in the LCPC body, these openings were filled by well-grown wardite crystals. A further growth of wardite was observed in 300 °C-autoclaved LCPC specimens. This filling up of the spacings by needle-like wardite crystals may serve to prevent a considerable loss in strength and an extremely high rate of water permeability.

Nevertheless, the LCPC specimens autoclaved at 300 °C for 24 h and derived from the slurry with a very low density of 0.98 $g\,cm^{-3}$ displayed a compressive strength of 2.3 MPa and a water permeability of 1.4×10^{-1} mdarcies. Moreover, when the LCPC specimens were exposed for up to 6 months to 0.05 M Na_2CO_3-laden solution at 250 °C, there was an increasing loss in strength during the first month of exposure; the loss gradually continued throughout 3 months, and then this decline seemed to level off. As a result, although the PAN-shelled microspheres were thermally decomposed near 200 °C, we believe that they have a better potential for use as light-weight filler of CPC slurry than chemically reactive inorganic ceramic or glass-shelled hollow microspheres because of the high reactivity of such inorganic microspheres with the Na ions from Na_2CO_3 solution at elevated temperatures, which causes the formation of a sponge-like porous structure after long-term exposure, thereby resulting in a serious loss in strength.

Acknowledgement

This work was performed under the auspices of the US Department of Energy, Washington, DC, under Contract DE-AC02-76CH00016.

References

1. T. SUGAMA and N. R. CARCIELLO, *Cem. Concr. Res.* **22** (1992) 783.
2. *Idem.*, *ibid.* **23** (1993) 1409.
3. T. SUGAMA, N. R. CARCIELLO, T. M. NAYBERG and L. E. BROTHERS, *ibid.* **25** (1995) 1305.
4. T. SUGAMA and N. R. CARCIELLO, *Adv. Cem. Based Mater.* **3** (1996) 45.
5. W. J. BURLANT and J. L. PARSONS, *J. Polym. Sci.* **22** (1956) 249.
6. A. R. MANAHAN, *J. Polym. Sci., Part A*-1 **4** (1966) 2391.
7. M. J. O'NEL, *Anal. Chem.* **36** (1964) 1238.
8. M. G. WYZGOSKI, *J. Appl. Polym. Sci.* **25** (1980) 1455.

Received 10 October 1995
and accepted 20 January 1997